Available online at www.sciencedirect.com
SCIENCE DIRECT®
Journal of Organometallic Chemistry 691 (2006) 1288–1294
Journal of Organometallic Chemistry
www.elsevier.com/locate/jorganchem

Reaction of the heteronuclear cluster $Cp^*IrOs_3(\mu\text{-}H)_4(CO)_9$ with alkynes: An unusual case of amine activation

Padmamalini Srinivasan, Jialin Tan, Weng Kee Leong *

Department of Chemistry, National University of Singapore, Kent Ridge, Singapore 119260, Singapore

Received 13 October 2005; received in revised form 2 December 2005; accepted 2 December 2005
Available online 9 January 2006

Abstract

Reaction of the heteronuclear cluster $Cp^*IrOs_3(\mu\text{-}H)_4(CO)_9$ with alkynes is activated by excess amine to afford the butterfly clusters $Cp^*IrOs_3(CO)_9(RCCR')$; hinge-apex isomers are formed. In the case of PhCCH, another cluster $Cp^*IrOs_3(CO)_9(CCHPh)_2$, which contained two alkenyl moieties was also isolated.

Keywords: Heterometallic complexes; Osmium; Iridium; Alkynes; Amine

1. Introduction

The reaction of tetrahedral clusters with alkynes most often leads to "butterfly" clusters [1], whereby the alkyne C_2 unit bonds to the metal framework in a μ_4–η^2 fashion to form a quasi-octahedral $M_3M'C_2$ skeleton [2]. For an unsymmetrical alkyne, three isomers are possible: The alkyne can be disposed parallel to a heterometallic MM′ bond or to a homometallic MM bond (these are related as hinge-apex isomers), and there are two different orientations of the alkyne with respect to the hinge bond (these are related as *cis–trans* alkyne isomers). The interaction of heteronuclear clusters with alkynes is of interest because of the possibility of stereoselective binding of the alkynes, which would be of great potential use in organic synthesis. For example, the reaction of $[CpMRu_3(CO)_{12}]^-$ (M = W, Mo), $IrRu_3(\mu\text{-}H)(CO)_{13}$ and $[IrRu_3(CO)_{13}]^-$ towards internal alkynes afforded ‖ M–Ru (M = W, Mo and Ir; ‖ M–Ru refers to the C≡C bond being parallel to the M–Ru bond) clusters with alkyne insertion into the Ru–Ru bond as the only product [3]. Similarly, the reaction of $Cp^*RhRu_3(\mu\text{-}H)_4(CO)_9$ with alkynes afforded the isomer with the heterometal atom at the wingtip (‖ Ru–Ru) as the only isomer. In contrast, however, the Cp analogue afforded both hinge-apex isomers (‖ Rh–Ru and ‖ Ru–Ru) [4].

Heterometallic clusters like $CpRhRu_3(\mu\text{-}H)_4(CO)_9$ are attractive as they allow not only studies on site selectivity in the binding of alkynes, particularly unsymmetrical alkynes, the Cp ligand also serves as a ligand which allows for additional stereochemical and electronic control on the cluster [4]. We have recently reported the reactivity with alkynes of a closely related system, viz., $Cp^*IrRu_3(\mu\text{-}H)_2(CO)_{10}$, in which stereoselective binding was observed [5]. In the course of that work, we also examined the analogous reactivity of $Cp^*IrOs_3(\mu\text{-}H)_2(CO)_{10}$ (**1**) and $Cp^*IrOs_3(\mu\text{-}H)_4(CO)_9$ (**2**). The mode of activation of the latter turned out to be rather unusual, which we are reporting here.

2. Results and discussion

The clusters **1** and **2** failed to react with excess alkyne even on heating to 120 °C. Photochemical activation (Hanovia lamp, 450 W, quartz vessel) afforded products in low yields. In both cases, some cluster fragmentation was also observed; $Cp^*Ir(CO)_2$ was detected spectroscopically, but

* Corresponding author.
E-mail address: chmlwk@nus.edu.sg (W.K. Leong).

0022-328X/$ - see front matter © 2005 Elsevier B.V. All rights reserved.
doi:10.1016/j.jorganchem.2005.12.006

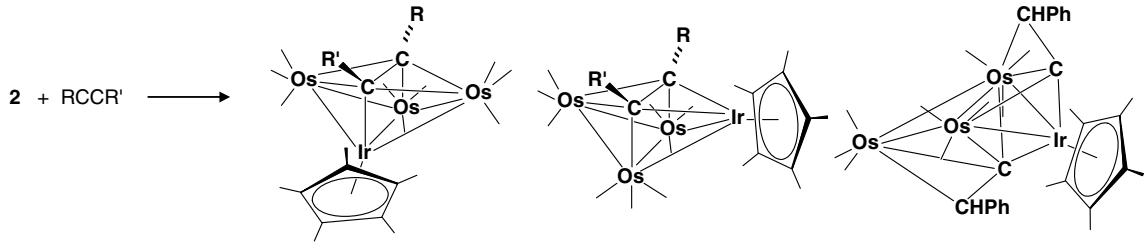

	3_1	3_2	4
a R = R' = Ph	26%	14%	
b R = R' = Et	1.7%	18%	
c R = Ph, R' = H	5%	not determined	10%

Scheme 1.

no triosmium species were isolated from the reactions. Initially, we had observed that chemical activation of **1** or **2** with excess TMNO afforded the clusters $Cp^*IrOs_3(CO)_9(RCCR)$ (**3**) in low yields. However, this did not seem very reasonable for **2** given that the usual mode of activation by TMNO is through the removal of a carbonyl ligand as CO_2 via O-atom transfer [6]. Furthermore, a large excess of TMNO was found to be required. We eventually realized that it could be trace amounts of amines in TMNO that may be responsible. Indeed, it turned out that **2** reacted with the alkynes in excess triethylamine as depicted in Scheme 1. With the exception of $\mathbf{3b_1}$ and $\mathbf{3c_2}$, the structures of all the clusters have been confirmed by single crystal X-ray crystallographic studies. In general, both hinge-apex isomers are obtained; the ORTEP plots for the diphenylacetylene derivatives $\mathbf{3a_1}$ and $\mathbf{3a_2}$ are give in Figs. 1 and 2, respectively.

In the case of phenylacetylene, the cluster $\mathbf{3c_2}$ was not separable chromatographically from another novel cluster, $Cp^*IrOs_3(CO)_9(CCHPh)_2$ (**4**); the crystals had to be separated mechanically, that of the former being red and the latter orange. The ORTEP plot of **4**, together with selected bond parameters, is shown in Fig. 3. The structure of **4**

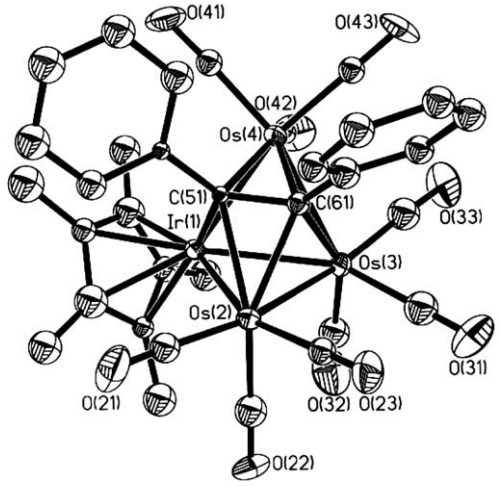

Fig. 1. ORTEP diagrams of $\mathbf{3a_1}$. Thermal ellipsoids are drawn at 50% probability level. Phenyl hydrogens are omitted for clarity.

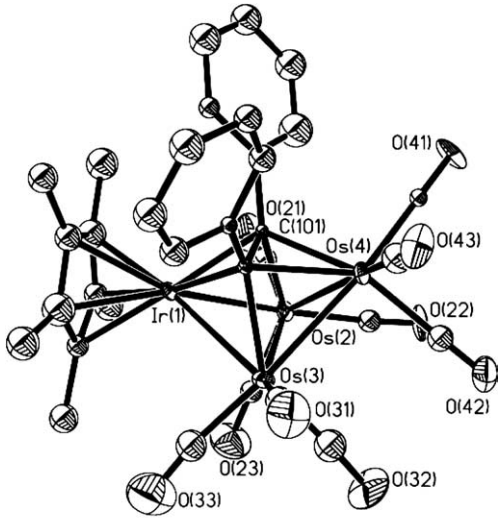

Fig. 2. ORTEP diagrams of $\mathbf{3a_2}$ (right). Thermal ellipsoids are drawn at 50% probability level. Phenyl hydrogens are omitted for clarity.

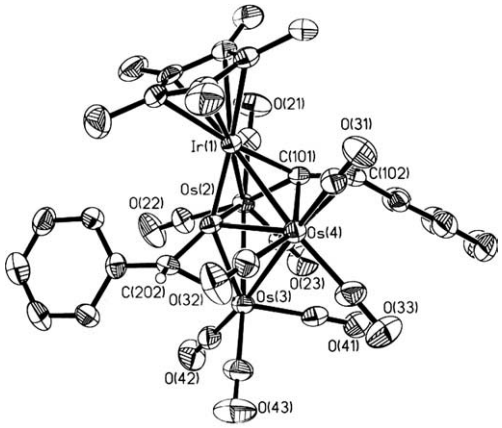

Fig. 3. ORTEP diagram and selected bond parameters of **4**. Thermal ellipsoids are drawn at 50% probability level. Aromatic hydrogens are omitted for clarity. Ir(1)–Os(4) = 2.7251(4) Å; Ir(1)–Os(2) = 2.7456(4) Å; Os(2)–Os(3) = 2.8594(4) Å; Os(3)–Os(4) = 2.8541(5) Å; Ir(1)–C(101) = 2.016(8) Å; Ir(1)–C(201) = 1.995(7) Å; Os(2)–C(101) = 2.096(8) Å; Os(2)–C(201) = 2.245(8) Å; Os(3)–C(201) = 2.159(7) Å; Os(3)–C(202) = 2.222(8) Å; Os(4)–C(101) = 2.330(8) Å; Os(4)–C(102) = 2.481(8) Å; Os(4)–C(201) = 2.381(8) Å; C(101)–C(102) = 1.356(11) Å; C(201)–C(202) = 1.443(10) Å; Ir(1)–Os(2)–Os(3) = 89.523(13)°; Ir(1)–Os(4)–Os(3) = 90.044(13)°.

consists of an Os_3Ir butterfly core. Two CCHPh units are found to be coordinated to the cluster core; one is bonded to all four metal atoms and the other to two osmium atoms and the iridium atom. These two units are best regarded as alkenyls although the C–C bond distances are fairly long (C(101)–C(102) = 1.356(11) Å; C(201)–C(202) = 1.443(10) Å) and are more consistent with single or at best partial double bond character [7]. The bonding involved in the CCHPh unit that is bonded to all the four metal atoms is interesting as the terminal carbon appears to form five bonds. However, the bond distances from this carbon atom to the two hinge osmium atoms, are considerably longer than to the wingtip atoms, suggesting that the bonds to the hinge atoms may have partial bond character. A reasonable picture of the bonding situation in **4** is that shown in Fig. 4.

A common atomic numbering scheme, and selected bond parameters, for clusters **3** are given in Table 1. The general structural features observed in the clusters **3** here are quite similar to those for the $IrRu_3$ analogues reported [5]. The alkyne is disposed parallel to the hinge metal–metal bond, with the torsion angle between the carbon–carbon backbone and the hinge close to 0°. This hinge M–M bond is also the longest of the metal–metal bonds, as has been generally found in M_4C_2 butterfly clusters [8]. The Ir–Os bond lengths in general are, however, comparable to Ir–Os bond distances reported in the literature [Ir–Os = 2.7759–2.906 Å] [9]. Also evident is the loss of multiple bond character in the alkyne C–C bond. This length is fairly consistent across the different clusters, averaging 1.45 Å and with the range of values well within the experimental errors, despite the variations in metal and substituents. The value is close to the 1.48 Å for carbon–carbon sp^2–sp^2 single bonds [7,10]. It is also clear that the alkyne is closer to the iridium than to the osmium, but this is consistent with the difference in the metal–metal bond lengths of $Ir_4(CO)_{12}$ and $Os_4(CO)_{12}$ (mean of 2.693 and 2.825 Å, respectively) [11].

The most intriguing aspect of this study, however, was the mechanistic role that the amine played in these reactions. Monitoring the reaction of **2** with triethylamine alone, or with triethylamine and alkyne, by infrared spectroscopy suggested that the reaction proceeded via an intermediate species. The IR spectral profile of this intermediate was similar to that of the pyridine-substituted derivative, $Cp^*IrOs_3(\mu\text{-}H)_2(CO)_9(py)$ (**5a**) obtained from the TMNO-activated reaction of **1** with pyridine [14]. Unfortunately, this intermediate species appeared to decompose during attempts at chromatographic purification. The reaction of **2** with PhCCPh and triethylamine, followed by ^1H NMR spectroscopy, suggested that *cis*-stilbene was formed in the reaction, in addition to $\mathbf{3a_1}$ and $\mathbf{3a_2}$. This would suggest that the loss of two hydrides from **2** was via hydrogenation of one equivalent of the alkyne; the stereochemistry of the product suggesting that both hydrogens came from metal hydride transfers. This form of activation, using an unsaturated hydrocarbon to effect hydride transfer, is known [12]. When **2** was first allowed to react with excess triethylamine followed by the addition of 1.0 equivalent of triphenylphosphine (after removal of the excess amine), the phosphine derivative $Cp^*IrOs_3(\mu\text{-}H)_2(CO)_9(PPh_3)$ (**5b**) [14], was obtained; **2** did not react directly with PPh_3, however. This result corroborated the existence of an intermediate, an amine derivative, with a structure similar to **5a**. We have thus tentatively formulated this intermediate as $Cp^*IrOs_3(\mu\text{-}H)_2(CO)_9(NEt_3)$ (**5c**). That **5b** could be formed without the presence of an alkyne indicated that the alkyne was not essential to the removal of the two hydrides. It is thus likely that the hydrides were lost as hydrogen, or were transferred to the alkyne if present; a proposed reaction pathway is given in Scheme 2.

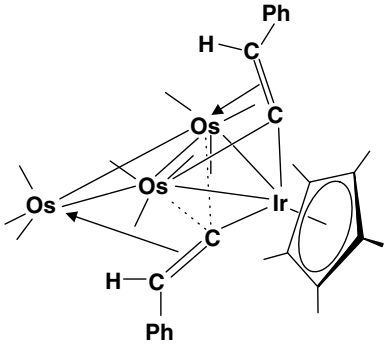

Fig. 4. Schematic of the bonding in **4**.

Table 1
Common atomic numbering scheme and selected bond lengths (Å) for $\mathbf{3a_1}$, $\mathbf{3a_2}$, $\mathbf{3b_2}$ and $\mathbf{3c_1}$

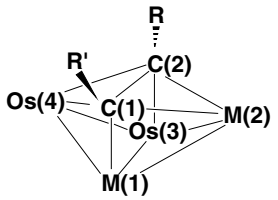

	$\mathbf{3a_1}$ R = R′ = Ph M(1) = Ir(1) M(2) = Os(2)	$\mathbf{3c_1}$ R = Ph R′ = H M(1) = Ir(1) M(2) = Os(2)	$\mathbf{3a_2}$ R = R′ = Ph M(1) = Os(1) M(2) = Ir(2)	$\mathbf{3b_2}$ R = R′ = Et M(1) = Os(1) M(2) = Ir(2)
M(1)–M(2)	2.6886(16)	2.6759(7)	2.6968(17)	2.7119(5)
M(1)–Os(3)	2.8048(16)	2.7940(7)	2.8356 (18)	2.8357(5)
M(1)–Os(4)	2.6510(16)	2.6561(7)	2.7672(17)	2.7617(5)
M(2)–Os(3)	2.7324(16)	2.7504(7)	2.7314(17)	2.7263(5)
Os(3)–Os(4)	2.7233(17)	2.7538(7)	2.7440(18)	2.7535(5)
M(1)–C(1)	2.15(2)	2.069(12)	2.19(3)	2.170(11)
M(2)–C(1)	2.30(2)	2.195(13)	2.17(3)	2.156(9)
Os(4)–C(1)	2.23(3)	2.177(13)	2.22(3)	2.264(9)
M(2)–C(2)	2.26(3)	2.274(11)	2.15(3)	2.152(9)
Os(3)–C(2)	2.18(3)	2.140(12)	2.15(3)	2.218(10)
Os(4)–C(2)	2.23(3)	2.224(12)	2.28(3)	2.249(9)
C(1)–C(2)	1.43(4)	1.446(16)	1.56(3)	1.458(15)

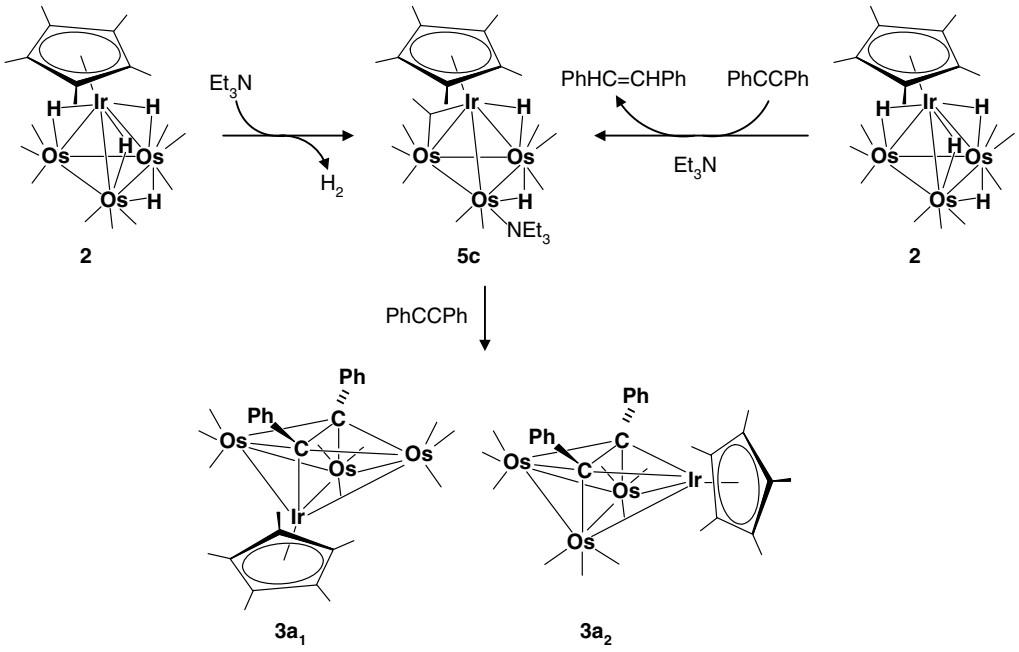

Scheme 2.

The observation of *cis*-stilbene in the reaction mentioned above also prompted us to carry out some preliminary investigations into the possibility of **2** acting as a catalyst for the hydrogenation of alkynes. Indeed, GC analysis of the mixture from the hydrogenation (40 psi) of diphenylacetylene with 2 mol% of **2** showed the presence of *cis*-stilbene, *trans*-stilbene, and bibenzyl. The cluster **2** remained unchanged and could be isolated by chromatographic separation. Similar results were also obtained with **1**.

3. Concluding remarks

Thus both **1** and **2** undergo alkyne insertion into the metal–metal bonds to afford alkyne substituted butterfly clusters; both hinge-apex isomers were obtained. The reaction is unusual in that it is activated by excess amine. The role of the amine appears to be to displace two hydrides and to form an unstable intermediate of formula Cp*Ir-$Os_3(\mu\text{-}H)_2(CO)_9(NEt_3)$.

4. Experimental

All reactions were carried out using standard Schlenk techniques under an atmosphere of nitrogen. Solvents used in reactions were of AR grade, and were dried, distilled and kept under argon in flasks fitted with Teflon valves prior to use. The products were generally separated by thin-layer chromatography (TLC), using plates coated with silica gel 60 F254 of 0.25 mm or 0.5 mm thickness and extracted with hexane or dichloromethane. Infrared spectra were recorded as hexane solutions unless otherwise stated on a Bio-Rad FTS 165 FTIR spectrometer at a resolution of 1 cm^{-1} using a solution cell with NaCl windows of path length 0.1 mm. NMR spectra were acquired on a Bruker ACF 300 MHz as C_6D_6 solutions unless otherwise stated. Chemical shifts reported are referenced to residual protons of the solvent.

Mass spectra were collected using the fast atom bombardment (FAB) technique and were carried out on a Finnigan MAT95XL-T mass spectrometer normally with 3-nitrobenzyl alcohol matrix at the National University of Singapore mass spectrometry laboratory. Microanalyses were carried out by the microanalytical laboratory at the National University of Singapore. GC analyses were carried out with an Agilent GC–MS consisting of a GC 6890 MS 5973 equipped with an HP-1 column (300 mm × 0.25 mm × 0.25 μm). In photochemical reactions, UV irradiation was performed with a Hanovia 450 W UV lamp ($\lambda_{max} = 254$ nm). The clusters **1** and **2** were prepared according to published procedures [13].

4.1. Reaction of 2 with alkynes

In a typical reaction, cluster **2** (10.0 mg, 9.0 μmol), PhCCPh (1.5 mg, 8.0 μmol) and hexane (20 ml) were placed in a Schlenk vessel. Excess triethylamine (1.5 ml) was then added to the solution which was then stirred at ambient temperature. The reaction was monitored by IR spectroscopy till completion (~21/2 h). The solvent was then removed under reduced pressure and the residue so obtained was redissolved in the minimum volume of dichloromethane and chromatographed on silica-gel TLC plates with hexane as eluant to afford two red bands of $\mathbf{3a_1}$ and $\mathbf{3a_2}$, in order of elution.

$\mathbf{3a_1}$: yield = 3.5 mg, 26%. IR (cm^{-1}): ν_{CO} 2071m, 2050vs, 2027s, 1993s, 1972mw, 1952w. ^1H NMR: 7.42–6.70 (m, 10H, Ph), 1.85 (s, 15H, Cp*). FAB^+-MS: m/z 1330 $[M]^+$.

Anal. Calc. for $C_{33}H_{25}IrO_9Os_3$: C, 29.84; H, 1.90. Found: C, 30.20; H, 2.00%.

3a$_2$: yield = 1.6 mg, 14%. IR (cm^{-1}): ν_{CO} 2077s, 2050w, 2036s, 2023vs, 2005mw, 1987w, 1979w, 1967w, 1954mw. ^1H NMR: 6.84–6.73 (m, 10H, Ph), 1.19 (s, 15H, Cp*). FAB^+-MS: *m/z* 1330 $[M]^+$. Anal. Calc. for $C_{33}H_{25}IrO_9Os_3$: C, 29.84; H, 1.90. Found: C, 30.18; H, 1.87.

An analogous procedure was followed for 3-hexyne and phenylacetylene to afford the following clusters.

3b$_1$: yield = 0.2 mg, 1.7%. IR (cm^{-1}): ν_{CO} 2066m, 2042vs, 2022s, 1985s, 1967ms, 1955w. FAB^+-MS: *m/z* 1232.7; calculated for $[M]^+ = 1232.3$.

3b$_2$: Yield = 2.1 mg, 18%. IR (cm^{-1}): ν_{CO} 2072s, 2032s, 2019vs, 1996mw, 1981m, 1976sh, 1963w, 1949ms. ^1H NMR: 3.16 (dq, $^2J_{HaHb} = 16$ Hz, $^3J_{HcHa} = 7.4$ Hz, 2H, $CH_{3c}CH_aH_bCCCH_aH_bCH_{3c}$) 2.48 (dq, $^2J_{HaHb} = 16$ Hz, $^3J_{HcHb} = 7.4$ Hz, 2H, $CH_{3c}CH_a\ H_bCCCH_a\ H_bCH_3$,), 1.28 (s, 15H, Cp*), 1.01 (dd, $^3J_{HcHa/Hb} = 7.4$ Hz, 6H, $CH_{3c}CH_aH_bCCCH_aH_bCH_{3c}$). FAB^+-MS: *m/z* 1232 $[M]^+$. Anal. Calc. for $C_{25}H_{25}IrO_9Os_3$: C, 24.37; H, 2.04. Found: C, 23.88; H, 1.81%.

3c$_1$: yield = 0.5 mg, 5%. IR (cm^{-1}): ν_{CO} 2071m, 2050vs, 2025s, 1993s, 1972m, 1954w. ^1H NMR: 11.32 (s, 1H, ≡CH), 7.42–6.73 (m, 5H, Ph), 1.89 (s, 15H, Cp*). FAB^+-MS: *m/z* 1252.2; calculated for $[M]^+ = 1252.2$.

3c$_2$: trace. IR (cm^{-1}): ν_{CO} 2076s, 2048w, 2035s, 2021vs, 2003m, 1986mw, 1972w, 1953w, 1948sh. FAB^+-MS: *m/z* 1252.2; calculated for $[M]^+ = 1252.2$.

4: yield = 1.2 mg, 10%. IR (CH_2Cl_2, cm^{-1}): ν_{CO} 2072m, 2046vs, 2029m, 1994ms, 1973br, 1960sh. ^1H NMR: 7.56–7.03 (m, 10H, Ph), 6.89 (s, 1H, =CH), 6.31 (s, 1H, =CH), 1.89 (s, 15H, Cp*). FAB^+-MS: *m/z* 1355 $[M]^+$. Anal. Calc. for $C_{35}H_{27}IrO_9Os_3$: C, 31.04; H, 2.01. Found: C, 31.04; H, 1.87%.

4.2. Reaction of *1* with PhCCPh

Cluster **1** (8.1 mg, 0.007 mmol) and PhCCPh (2.6 mg, 0.015 mmol) were dissolved in CH_2Cl_2 (15 ml). TMNO (1.5 mg, 0.021 mmol) in CH_2Cl_2 (10 ml) was added dropwise at room temperature. After stirring for 3 h, the IR spectrum of the mixture showed no change.

A similar reaction with excess Et_3N (1.5 ml) in place of TMNO, and hexane (5 ml) as solvent afforded, after 4 h and TLC separation, mainly unreacted **1** and a trace of **3a$_1$**.

In another reaction, **1** (10 mg, 8.0 μmol), PhCCPh (1.5 mg, 8.0 μmol), triethylamine (1.5 ml) and TMNO (0.8 mg, 8.0 μmol), were stirred in hexane at ambient temperature for 20 min. After removal of the solvent under reduced pressure and TLC separation (hexane as eluant), **3a$_1$** (1.2 mg, 10%) and **3a$_2$** (2.8 mg, 24%) were obtained (identified from their IR spectra).

4.3. Reaction of *2* with PhCCPh in the presence of TMNO

To a Schlenk flask containing **2** (20.6 mg, 18.0 μmol) and PhCCPh (1.5 mg, 8.0 μmol) in dichloromethane was added TMNO (3.9 mg, 54 μmol) dissolved in dichloromethane (15 ml) through a dropping funnel. The reaction mixture stirred at ambient temperature for 21/2 h, the solvent was removed under reduced pressure, and the residue redissolved in the minimum volume of hexane and subjected to TLC on silica-gel plates. Elution with hexane afforded **3a$_1$** and **3a$_2$**, in 3% and 5% yields, respectively.

4.4. Reaction of *2* with triethylamine

To a Schlenk flask containing **2** (10 mg, 9.0 μmol) in hexane (5 ml) was added triethylamine (1.5 ml, 10.8 mmol), and the reaction mixture stirred for 2 h at room temperature. The IR spectrum showed the presence of an intermediate species, with ν_{CO} 2066m, 2040vs, 1996s, 1967sh, 1942sh and 1701br cm^{-1}, and the ^1H NMR spectrum showed resonances at δ 1.92 (s, 15H, Cp*) and −18.85 (s, 2H, OsHOs). Removal of the solvent under reduced pressure followed by TLC on silica-gel plates afforded two bands. The fast moving band was identified as **1** (1.1 mg, 13%) from its IR spectrum. The second band (2.5 mg) gave the following spectroscopic characteristics: IR: ν_{CO} 2079w, 2065s, 2040vs, 1996vs, 1966s, 1941w, 1701br cm^{-1}. ^1H NMR: δ 1.92 (s, 15H, Cp*), −18.86 (s, 1H, OsHOs), −17.36 (s, 1H, OsHOs).

4.5. Reaction of *2* with PPh_3

To a Schlenk flask containing **2** (8 mg, 7.0 μmol) in dichloromethane was added triethylamine (1.5 ml, 10.8 mmol) and the reaction mixture stirred for 2 h at ambient temperature. The solvent and excess triethylamine were removed under reduced pressure. The residue was redissolved in dichloromethane (10 ml) and triphenyl phosphine (1.8 mg, 7.0 μmol) was added, and the reaction mixture stirred for 1 h. TLC separation on silica-gel plates with 100% hexane afforded **5b** as the major product, identified from its IR spectrum [14]. Yield = 5 mg, 51%.

4.6. Reaction of *1* or *2* with PhCCPh under hydrogen

To a Parr bomb of 60 ml capacity fitted with a glass-lining were added **1** (5 mg, 4 μmol) and PhCCPh (37.7 mg, 210 μmol). Octane (2 ml) was added and the solution was purged with nitrogen for 5 min. The bomb was then fitted with a gauge, flushed three times with H_2, pressurized to 40 psi, and the contents heated at 120 °C for 1 h. The reaction mixture was then cooled, transferred to a round-bottomed flask, and the solvent removed under reduced pressure. The residue obtained was redissolved in hexane and subjected to TLC with 100% hexane as eluant. The colourless, fast moving, broad band was identified as a mixture of *cis*-stilbene, *trans*-stilbene and bibenzyl by GC analysis. The identities of these compounds were further confirmed by ^1H NMR spectroscopy. Cluster **1** (3.5 mg) was recovered, as identified by its IR spectrum. Similar results were obtained with **2** in place of **1**.

Table 2
Crystal and refinement data for **3a$_1$**, **3a$_2$**, **3b$_2$**, **3c$_1$** and **4**

Compound	**3a$_1$**	**3a$_2$**	**3b$_2$**	**3c$_1$**	**4**
Empirical formula	$C_{33}H_{25}IrO_9Os_3$	$C_{33}H_{25}IrO_9Os_3$	$C_{25}H_{25}IrO_9Os_3$	$C_{27}H_{21}IrO_9Os_3$	$C_{35}H_{27}IrO_9Os_3$
Formula weight	1328.33	1328.33	1232.25	1252.24	1354.37
Crystal system	Monoclinic	Monoclinic	Orthorhombic	Monoclinic	Monoclinic
Space group	$P2_1/c$	$P2_1/c$	$Pna2_1$	$P2_1/n$	$P2_1/c$
Unit cell dimensions					
a (Å)	14.0473(11)	10.461(2)	20.7574(5)	10.6110(3)	10.3772(6)
b (Å)	9.6988(8)	16.140(3)	8.6815(2)	19.1640(5)	18.6177(10)
c (Å)	24.0120(19)	20.075(4)	15.3589(4)	28.3928(8)	18.5247(10)
α (°)	90	90	90	90	90
β (°)	92.335(2)	104.498(6)	90	93.7540(10)	100.8490(10)
γ (°)	90	90	90	90	90
Volume (Å^3)	3268.7(5)	3281.6(11)	2767.76(12)	5761.3(3)	3515.0(3)
Z	4	4	4	8	4
ρ (calc) (Mg/m^3)	2.699	2.689	2.957	2.887	2.559
Absorption coefficient (mm^{-1})	15.736	15.674	18.570	17.846	14.636
$F(000)$	2400	2400	2208	4480	2456
Crystal size (mm^3)	$0.18 \times 0.06 \times 0.04$	$0.14 \times 0.06 \times 0.02$	$0.20 \times 0.16 \times 0.10$	$0.14 \times 0.09 \times 0.04$	$0.30 \times 0.22 \times 0.20$
Theta range for data collection	2.19–26.37°	2.10–26.37°	2.37–29.64°	2.01–26.37°	2.00–26.37°
Reflections collected	45 562	21 242	23 601	78 947	32 453
Independent reflections [R_{int}]	6666 [0.0771]	6686 [0.1244]	3801 [0.0449]	11 788 [0.0873]	7179 [0.0502]
Data/restraints/parameters	6666/6/255	6686/54/243	3801/1/350	11788/15/719	7179/1/444
Goodness-of-fit on F^2	1.245	1.206	1.017	1.110	1.035
Final R indices [$I > 2\sigma(I)$]	$R_1 = 0.0953$	$R_1 = 0.1186$	$R_1 = 0.0256$	$R_1 = 0.0497$	$R_1 = 0.0348$
	$wR_2 = 0.2297$	$wR_2 = 0.2206$	$wR_2 = 0.0551$	$wR_2 = 0.1005$	$wR_2 = 0.0727$
R indices (all data)	$R_1 = 0.1035$	$R_1 = 0.1532$	$R_1 = 0.0280$	$R_1 = 0.0705$	$R_1 = 0.0482$
	$wR_2 = 0.2331$	$wR_2 = 0.2364$	$wR_2 = 0.0559$	$wR_2 = 0.1080$	$wR_2 = 0.0777$
Largest difference in peak and hole (e Å^{-3})	6.610 and −3.538	6.247 and −3.605	1.858 and −1.115	4.693 and −1.723	1.442 and −0.853

4.7. X-ray crystal structure determinations

Diffraction quality crystals were grown from hexane by slow cooling. Crystals were mounted on quartz fibres. X-ray data were collected on a Bruker AXS APEX system, using Mo Kα radiation, at 223 K with the SMART suite of programs [15]. Data were processed and corrected for Lorentz and polarization effects with SAINT [16], and for absorption effects with SADABS [17]. Structural solution and refinement were carried out with the SHELXTL suite of programs [18]. Crystal and refinement data are summarized in Table 2.

The structures were solved by direct methods to locate the heavy atoms, followed by difference maps for the light, non-hydrogen atoms. All non-hydrogen atoms were generally given anisotropic displacement parameters in the final model. Organic hydrogen atoms were placed in calculated positions and refined with a riding model. Compound **3b$_2$** was refined as a racemic twin. There were two crystallographically independent molecules in **3c$_1$**, one of which showed a badly behaved phenyl ring, on which vibration and bond length restraints were placed. Restraints were also employed on **3a$_1$** and **3a$_2$**.

Acknowledgements

This work was supported by the National University of Singapore (Research Grant No. R143-000-190-112) and one of us (P.S.) thanks the University for a Research Scholarship.

Appendix A. Supplementary information available

CCDC 283351–283355 contains the supplementary crystallographic data for this paper. These data can be obtained free of charge from The Cambridge Crystallographic Data Centre via www.ccdc.cam.ac.uk/data_request/cif. Supplementary data associated with this article can be found, in the online version, at doi:10.1016/j.jorganchem.2005.12.006.

References

[1] E. Sappa, A. Tiripicchio, A.J. Carty, G.E. Toogood, Prog. Inorg. Chem. 35 (1987) 437.
[2] (a) E.W. Abel, F.G.A. Stone, G. Wilkinson, Comprehensive Organometallic Chemistry II, first ed., Pergamon, Oxford, New York, 1995;
(b) L.F. Dahl, D.L. Smith, J. Am. Chem. Soc. 84 (1962) 2450;
(c) R.J. Haines, N.D.C.T. Steen, M. Laing, P. Sommerville, J. Organomet. Chem. 198 (1980) C72.
[3] (a) M. Cazanoue, N. Lugan, J.J. Bonnet, R. Mathieu, Organometallics 7 (1988) 2480;
(b) V. Ferrand, G. Süss-Fink, A. Neels, H. Stoeckli-Evans, J. Chem. Soc., Dalton Trans. (1998) 3825;
(c) V. Ferrand, G. Süss-Fink, A. Neels, H. Stoeckli-Evans, Eur. J. Inorg. Chem. (1999) 853.
[4] J.L. Le Grand, W.E. Lindsell, K.J. McCullough, C.H. McIntosh, A.G. Meiklejohn, J. Chem. Soc., Dalton Trans. (1992) 1089.
[5] P. Srinivasan, W.K. Leong, Eur. J. Inorg. Chem. (in press).
[6] For examples, see: (a) N.E. Leadbeater, C. van der Pol, J. Chem. Soc., Chem. Commun. (2001) 599;
(b) J.K. Shen, Y.C. Gao, Q.Z. Shi, F. Basolo, J. Organomet. Chem. 401 (1991) 295;

(c) U. Koelle, J. Organomet. Chem. 155 (1978) 53;
(d) U. Koelle, J. Organomet. Chem. 133 (1977) 53.
[7] M. Smith, J. March, March's Advanced Organic Chemistry: Reactions, Mechanisms and Structure, fifth ed., Wiley, New York, Singapore, 2001.
[8] (a) S. Haak, G. Süss-Fink, A. Neels, H. Stoeckli-Evans, Polyhedron 18 (1999) 1675;
(b) G. Süss-Fink, S. Haak, V. Ferrand, H. Stoeckli-Evans, J. Chem. Soc., Dalton Trans. (1997) 3861.
[9] (a) A. Fumagalli, M.C. Malatesta, M. Vallario, G. Ciani, M. Moret, A. Sironi, J. Cluster Sci. 12 (2001) 187;
(b) H.C. Bottcher, M. Graf, K. Merzweiler, C. Wagner, Polyhedron 19 (2000) 2593;
(c) G. Süss-Fink, S. Haak, V. Ferrand, H. Stoeckli-Evans, J. Mol. Catal. A 143 (1999) 163;
(d) J.R. Galsworthy, C.E. Housecroft, D.M. Matthews, R. Ostrander, A.L. Rheingold, J. Chem. Soc., Dalton Trans. (1994) 69;
(e) L.Y. Hsu, W.L. Hsu, D.A. McCarthy, J.A. Krause, J.H. Chung, S.G. Shore, J. Organomet. Chem. 426 (1992) 121.
[10] (a) B.F.G. Johnson, J. Lewis, B.E. Reichert, K.T. Schorpp, G.M. Sheldrick, J. Chem. Soc., Dalton Trans. (1977) 1417;
(b) P.R. Raithby, M.J. Rosales, Adv. Inorg. Chem. Radiochem. 29 (1985) 169.
[11] (a) V.J. Johnston, F.W.B. Einstein, R.K. Pomeroy, Organometallics 7 (1988) 1867;
(b) M.R. Churchill, J.P. Hutchinson, Inorg. Chem. 17 (1978) 3528;
(c) M.R. Churchill, F.J. Hollander, J.P. Hutchinson, Inorg. Chem. 16 (1977) 2655.
[12] For examples, see: (a) A.D. Selmeczy, W.D. Jones, Inorg. Chim. Acta 300–302 (2000) 138;
(b) G.E. Herberich, W. Barlage, K. Linn, J. Organomet. Chem. 414 (1991) 193;
(c) M. Tachikawa, J.R. Shapley, J. Organomet. Chem. 124 (1977) C19.
[13] P. Srinivasan, W.K. Leong, J. Organomet. Chem. (in press).
[14] P. Srinivasan, Leong, J. Organomet. Chem. (in press).
[15] SMART version 5.628, Bruker AXS Inc., Madison, WI, USA, 2001.
[16] SAINT+ version 6.22a, Bruker AXS Inc., Madison, WI, USA, 2001.
[17] G.M. Sheldrick, SADABS, 1996.
[18] SHELXTL version 5.1, Bruker AXS Inc., Madison, WI, USA, 1997.